ON THE 4-POINT CONDUCTANCE OF GRAPHENE NANORIBBONS

Martin Konôpka, Peter Dieška

SLOVAK UNIVERSITY OF TECHNOLOGY in Bratislava
Faculty of Electrical Engineering and Information Technology
Institute of Nuclear and Physical Engineering
Department of Physics
Ilkovičova 3, 812 19 Bratislava, Slovak Republic
E-mail: martin.konopka@stuba.sk

Received 29 April 2017; accepted 25 May 2017

1. Introduction

Many of the proposed graphene-based devices utilise its unique electronic properties [1]. Recently graphene nanoribbons (GNRs) have been proposed to provide a functionality analogous to optical fibres [2]. The operation of such device would be based on electronic states localised closed to its edges. The electric current is expected to flow along the ribbon edge analogously to light through a fibre. Since such a setup would require an electrical contact of the GNR to the rest of the scheme, a natural question about electrical conductance properties of corner-contacted GNRs emerges. Similar contacts have been computationally studied in Ref. [3] where the main focus have been non-rectangular graphene flakes with two electrodes attached at it. Recently we turned our attention to (rectangular) GNRs with the aim to study a setup with two constant electric currents flowing along the two parallel edges of a nanoribbon [4]. This led us to consider a 4-terminal device in the ballistic regime and explore its properties with the aid of the Landauer-Büttiker (LB) multiterminal formalism. We proposed a scheme with two classical electrical circuits characterised by their resistances and bias voltage sources and coupled through the quantum device – the GNR-based nanojunction which is in turn characterised by its conductance matrix. The studied model was a generalisation of the Büttiker's resistance-free model [5]. The currents in the two circuits were found to influence each other in general. Such a coupling of the classical devices through a quantum one is certainly an intriguing phenomenon from the physical point of view. On the other hand, we studied also the regime in which the currents in the two circuits can flow almost independently, i.e. mutually almost decoupled. The weak mutual coupling would make possible to employ a single nanoribbon to serve as two almost independent conductors. A scheme with such GNR-based conductors might allow to shrink the size of a nano-electronic device using the conductors. Whether the operation of the two circuits is sufficiently independent or not depends on the conductance matrix of the nanojunction.

In this contribution we provide our preliminary computational results on the 4-point conductance properties of GNR-based nanojunctions. We assume defect-free GNRs at zero or low temperatures and study how their ballistic conductance depends on the GNR's dimensions. We note that in recent years advances in nanotechnology allowed to fabricate atomically precise GNRs [6] so that defect-free GNRs are not merely an idealisation. Among our results we determine an optimal GNR size which in the low temperature limit provides maximal values of the computed four-point electrical conductance matrix elements.

2. The studied model

We study several tens of graphene samples of the rectangular shape – the graphene nanoribbons. A sample structure is shown on Fig. 1. For the purpose of the computational

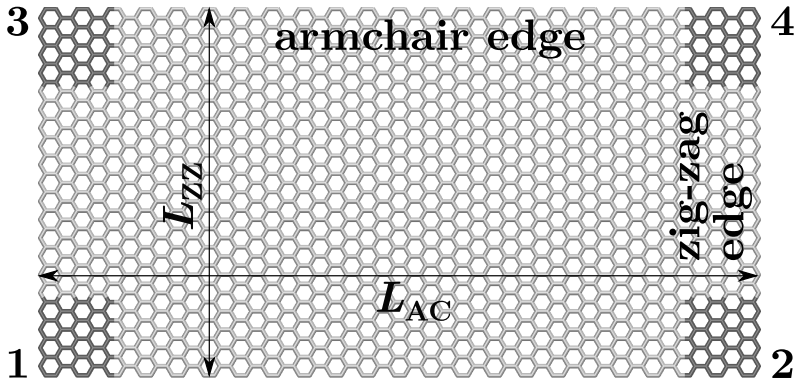

Fig. 1: *Illustration of a GNR with four electrical contacts. The dark-coloured corner areas represent those atoms to which the electrodes are coupled. The numerical labels at the corners define the indexing used in the formal description in formulae like* (1)*. The size of the particular sample on the figure along the armchair-edge direction* $L_{\mathrm{AC}} = 68\,a \approx 9.656\,\mathrm{nm}$*, where* $a \approx 0.142\,\mathrm{nm}$ *is the nearest-neighbour distance in graphene. Similarly the size along the the zig-zag direction* $L_{\mathrm{ZZ}} = 20\,b \approx 4.919\,\mathrm{nm}$ *with the lattice parameter* $b \equiv a\sqrt{3}$*. The total number of atoms of the displayed sample is* 1866*.*

model the electrodes (not shown in the figure) are composed of a bunch of semi-infinite monoatomically thin mutually non-interacting wires. Models of this kind were used and are described also in Refs. [7, 3]. In the present work we employ 45 wires per electrode. The whole system including the GNR and the electrodes is assumed at a negligible temperature. Its description is necessarily quantum-mechanical and in our model it is based on the independent-electron model and a tight-binding (TB) hamiltonian with extended couplings. One orbital per atom is considered. The nearest-neighbour (NN) distance of the atoms in the GNR is $a \approx 0.142\,\mathrm{nm}$. The couplings of the atoms both in the GNR and in the wires are quantified by a TB hopping parameter $t_{\mathrm{B}} \approx -2.97\,\mathrm{eV}$. While the model based on the basic TB hamiltonian has proven itself to be sufficiently accurate for many studies [1], we have found in our work [3] that it fails to describe the conductance properties of GNR junctions if the corners serve as contact areas. Therefore we include interactions up to the 3^{rd} NN within the GNRs, with the two additional parameters $t'_{\mathrm{B}} = -0.073\,\mathrm{eV}$ and $t''_{\mathrm{B}} = -0.33\,\mathrm{eV}$ [8]. The interactions within the wires are considered up to the 2^{nd} NN using again the parameters t_{B} and t'_{B}. The interaction between the GNR and the wires is described by the parameters t_{B} and t'_{B} as well. The conductance matrix is calculated for the ballistic regime which is realistic at low temperatures. We use the standard Green's function formalism to obtain electronic wavefunctions [9] and consequently the conductance matrix. Apart from the presently used extension (see Ref. [4] for its details) of the TB model of the wires, the electronic structure and the conductance matrix calculations are performed in the same way as in Ref. [3].

If the four terminals of the device are coupled to reservoirs of different electrochemical (hence also electrostatic) potentials, an electric current is built up. We assume a linear-response (low voltage) regime in which

$$I_\alpha \;=\; \sum_{\substack{\beta=1\\ \beta\neq\alpha}}^{4} G_{\alpha\beta}\,.\,(U_\alpha - U_\beta)\,, \qquad \alpha \in \{1,\ldots,4\} \tag{1}$$

is the current flowing through the electrode α [5]. U_γ are the electrostatic potentials of the four electrodes and $G_{\alpha\beta}$ are the conductance matrix elements, assumed to be energy-independent in the linear regime. We assume zero magnetic field and neglect spin-related effects. The low-voltage regime allows us to compute the conductance matrices at the equilibrium Fermi energy only.

3. Results

The conductance matrix in general obeys to the time-reversal symmetry rule $\sum_\beta G_{\alpha\beta} = \sum_\beta G_{\beta\alpha}$ For we assume zero magnetic field the matrix simplifies to a symmetric form [5]. In addition, the geometrical symmetry of the rectangular GNRs such as the one shown in Fig. 1 yields the relations

$$G_{12} = G_{34} \equiv G_{\mathrm{AC}}\,, \qquad G_{13} = G_{24} \equiv G_{\mathrm{ZZ}}\,, \qquad G_{14} = G_{23} \equiv G_{\mathrm{X}} \tag{2}$$

The numerical indices correspond to the indexing of the four corners defined in Fig. 1. The symbols G_{AC}, G_{ZZ} and G_{X} denote the conductances associated with the armchair (AC) direction, the zig-zag (ZZ) direction and the diagonal (X) directions. Under the assumed conditions the ballistic conductance properties of a GNR are thus completely described by the three off-diagonal elements of the matrix G We compute the conductance matrices for several tens of GNRs differing by their sizes L_{AC} and L_{ZZ} (see Fig. 1). We note that all of them have L_{ZZ} sizes corresponding to conductive (or metallic) armchair GNRs [10]. First we show (Fig. 2) how the conductance depends on the sample length along the AC direction. The striking feature

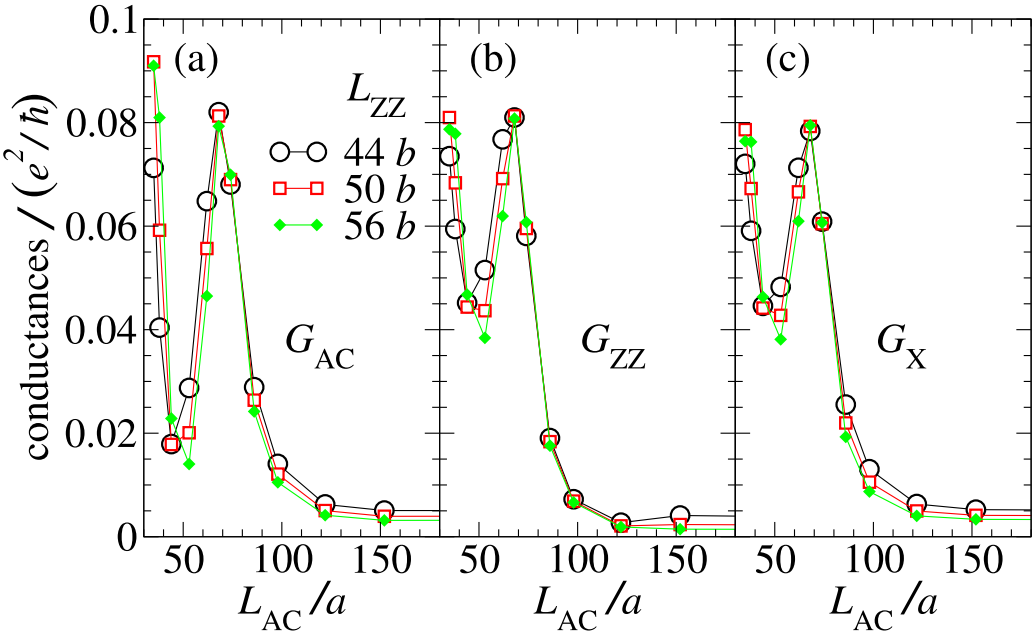

Fig. 2: *The three different off-diagonal elements of the conductance matrix plotted as functions of the GNR's size (the length) L_{AC} for the three different widths $L_{\mathrm{ZZ}} \in \{44, 50, 56\}\, b \approx \{10.82, 12.30, 13.77\}$ nm; see the caption to Fig. 1 for information on the parameters a and b. The legends related to the L_{ZZ} values apply to all three panes. (a), (b), (c): The conductances associated with the AC, ZZ, and X directions, respectively, as defined by the Eq.* (2).

is that all three matrix elements exhibit qualitatively similar dependence on L_{AC}. At first sight

this may be a counterintuitive result. The similar features can be comprehended as resulting from the electronic structure of the nanojunction and from its symmetry. The spectrum of the junction's eigenstates yields similar probabilities for an electron to tunnel from a given terminal to any of the remaining three terminals. A minor exception is the dip around $L_{\mathrm{AC}} = 44\,a$ which is deeper for G_{AC} than for the other two conductances.

In addition to the dip, the interesting feature are the peaks at about $L_{\mathrm{AC}} = 68\,a$. It is not surprising that short GNRs are characterised by the large conductances as it is seen from the Fig. 2. Such short GNRs may not be practical for an experimental realisation. However the single peak in all the plots mean that there is an optimal length (about $68\,a$) for a GNR to provide maximum conductance. We have data available for even longer GNRs and they show just very weakly varying, practically constant $G_{\alpha\beta}$ matrix elements at larger GNRs' lengths.

The results in Fig. 2 display a marginal dependence on the GNR's size L_{ZZ} along the ZZ direction. We performed a set of calculations for ribbons of the length $L_{\mathrm{AC}} = 68\,a$, i.e. for

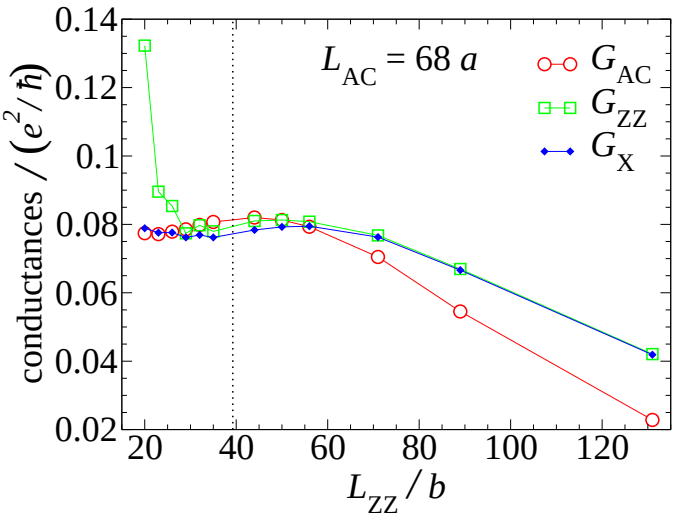

Fig. 3: *The three different off-diagonal elements of the conductance matrix plotted as functions of the GNR's size (the width) L_{ZZ} for GNRs of the length $L_{\mathrm{AC}} = 68\,a \approx 9.656\,\mathrm{nm}$; see the caption to Fig. 1 for information on the parameters a and b. The other symbols are explained in the caption to Fig. 2. The vertical dotted line marks the magnitude of L_{ZZ} corresponding to a square-shaped GNR.*

the length providing the peak of conductances. The $G_{\alpha\beta}$ plots vs. the width L_{ZZ} are shown in Fig. 3. Not surprisingly, the G_{ZZ} conductance becomes very high for the GNRs of the short L_{ZZ} sizes. The coincidence of G_{AC} with G_{X} for samples narrow along the ZZ direction is also intuitively clear. The same is true for the coincidence of G_{ZZ} with G_{X} for wide samples.

While the conductances practically saturate at a non-vanishing value in the limit of the large L_{AC} size (Fig. 2), they monotonously decrease if the perpendicular size L_{ZZ} increases (Fig. 3), an observation seen for the computed sizes up to $263\,b$ (beyond the scale shown in Fig. 3). Partially similar results are found also for $G_{\alpha\beta}$ vs. L_{ZZ} computed for a longer set of GNRs ($L_{\mathrm{AC}} = 86\,a$, not shown in graphs). The $L_{\mathrm{AC}} = 86\,a$ structures do not yield the wide local maxima in the $G_{\alpha\beta}$ vs. L_{ZZ} plots. In overall, we can say that beyond the local maxima the conductances get lower or saturate at a finite value as the number of the composing atoms increases.

4. Conclusion

In this computational work we studied the 4-point electrical conductance $G_{\alpha\beta}$ of GNRs contacted at their corners. The motivation of this work comes from considerations about GNR's edges functioning analogously to optical fibres [2]. Our recent work [3] was probably the first one in which corners of graphene flakes were considered as contact areas. In the present contribution we have extended these ideas to ordinary rectangular GNRs. We consider approximately square (about $0.9 \times 1\,\mathrm{nm}^2$) contacts. Our preliminary results in this contribution show that there are optimal GNR dimensions such those yield maxima of the conductances. The optimal size is about $L_{\mathrm{AC}}^{\mathrm{opt}} \approx 9.656\,\mathrm{nm}$ along the armchair direction and about $L_{\mathrm{ZZ}}^{\mathrm{opt}} \approx 12.3\,\mathrm{nm}$ along the zigzag direction; the variation of $G_{\alpha\beta}$ with the L_{ZZ} size is relatively weak. The conductance matrix elements at larger L_{AC} slowly decrease and saturate at a non-vanishing value. The dependence on the L_{ZZ} size exhibits more differences between different matrix elements, with the common feature that beyond $L_{\mathrm{ZZ}}^{\mathrm{opt}}$ they all decrease for the studied range of the L_{ZZ} sizes. Among several open questions, a comparison to the 2-point conductance as well as the effect of the contact size areas may be addressed in a future work.

Acknowledgement

This work was supported in parts by the Slovak Research and Development Agency under the contract No. APVV-0108-11 and by the Slovak Grant Agency for Science (VEGA) through grants No. 1/0372/13 and 2/0152/16. The GNR structure was visualised using VMD [11].

References:

[1] A.H. Castro Neto, F. Guinea, N.M.R. Peres, K.S. Novoselov, A.K. Geim, *Rev. Mod. Phys.* **81**, 109 (2009).

[2] M.T. Allen O. Shtanko, I.C. Fulga, A.R. Akhmerov, K. Watanabe, T. Taniguchi, P. Jarillo-Herrero, L.S. Levitov, A. Yacoby, *Nature Physics* **12**, 128 (2016).

[3] M. Konôpka, *J. Phys.: Condens. Matter.* **27**, 435005 (2015).

[4] M. Konôpka, Peter Dieška, `http://arxiv.org/abs/1701.03815`, in preparation.

[5] M. Büttiker, *Phys. Rev. Lett.* **14**, 1761 (1986).

[6] J. Cai et al., *Nature* **466**, 470 (2010).

[7] M. Konôpka, P. Bokes, *Phys. Rev. B* **89**, 125424 (2014).

[8] S. Reich, J. Maultzsch, C. Thomsen, P. Ordejón, *Phys. Rev. B* **66**, 035412 (2002).

[9] D.A. Ryndyk, B. Song, R. Gutiérrez, G. Cuniberti, *Green Function Techniques in the Treatment of Quantum Transport at the Molecular Scale*, in Energy Transfer Dynamics in Biomaterial Systems, edited by I. Burghardt, V. May, D.A. Micha, E. Bittner, Springer Series in Chemical Physics Vol. 93 (Springer-Verlag, Berlin, Heidelberg, 2009), p. 213.

[10] Y.-W. Son, M.L. Cohen, S.G. Louie, *Phys. Rev. Lett.* **97**, 216803 (2006).

[11] W. Humphrey, A. Dalke, K. Schulten, *J. Molec. Graphics* **14**, 33 (1996).